

## **Integrating an Energy Storage Device with STATCOM to Reduce Power Oscillation Damping**

**Y.Sai Krishna**

**M.Tech Student Scholar,  
Dept of EEE,**

**Audisankara College of Engineering & Technology  
(Autonomous) Gudur, Spsr Nellore (Dt), A.P.**

**B.Anil Kumar, M.Tech, MISTE**

**Assistant Professor,  
Dept. of EEE,**

**Audisankara College of Engineering & Technology  
(Autonomous) Gudur, Spsr Nellore (Dt), A.P.**

### **ABSTRACT:**

This paper offers with the layout of an adaptive power oscillation damping (POD) controller for a static synchronous compensator (STATCOM) set with energy storage. This is carried out the usage of a signal estimation technique based totally on a changed recursive least square (RLS) algorithm, which lets in a fast, selective, and adaptive estimation of the low-frequency electromechanical oscillations from locally measured signals at some stage in power gadget disturbances. The proposed technique is effective in growing the damping of the device at the frequencies of interest, additionally within the case of machine parameter uncertainties and at diverse connection factors of the compensator. First, the analysis of the effect of active and reactive energy injection into the energy gadget can be accomplished the usage of a simple device machine model.

A manipulate approach that optimizes energetic and reactive strength injection at numerous connection points of the STATCOM will be derived the usage of the simplified version. Small-signal evaluation of the dynamic overall performance of the proposed manage strategy might be completed. The effectiveness of the proposed control approach to offer strength oscillation damping no matter the connection point of the tool and in the presence of system parameter uncertainties will be established through simulation outcomes.

### **1. INTRODUCTION:**

Static synchronous compensator (STATCOM) is a key tool for reinforcement of the stableness in an ac power system. This device has been applied both at distribution level to mitigate power quality phenomena and at transmission degree for voltage manage and power oscillation damping (POD) [1]–[3]. Even though typically used for reactive power injection handiest, by using equipping the STATCOM with an energy garage connected to the dc-link of the converter, a more flexible manipulate of the transmission machine can be finished [4], [5]. An installation of a STATCOM with power storage is already observed within the U.K. for power go with the flow management and voltage control [6].

The creation of wind electricity and different dispensed generation will pave the way for more energy storage into the strength system and auxiliary stability enhancement characteristic is possible from the power sources [7]. Because injection of active power is used temporarily for the duration of brief, incorporating the steadiness enhancement function in structures in which active strength injection is mainly used for different functions [8] can be attractive. Low-frequency electromechanical oscillations (normally in the variety of 0.2 to 2 Hz) are not unusual in the electricity machine and are a purpose for situation regarding comfy machine operation, especially in a vulnerable transmission gadget [9].

In this regard, information controllers, both in shunt and collection configuration, were broadly used to beautify stability of the power system [1]. Within the specific case of shunt connected records controllers [STATCOM and static var compensator (SVC)], first swing stability and POD can be finished with the aid of modulating the voltage at the point of common coupling (percent) the usage of reactive power injection. However, one downside of the shunt configuration for this type of packages is that the PCC voltage have to be regulated inside specific limits (generally between  $\pm 10\%$  of the rated voltage), and this reduces the amount of damping that could be furnished by the compensator. Moreover, the amount of injected reactive electricity had to modulate the percent voltage depends on the quick circuit impedance of the grid seen at the connection point. Injection of lively strength, however, impacts the PCC-voltage attitude (transmission lines are efficiently reactive) without various the voltage importance drastically. The manipulate of STATCOM with strength storage (named hereafter as E-STATCOM) for power system balance enhancement has been mentioned within the literature [10]–[12].

But, the impact of the region of the E-STATCOM on its dynamic performance is normally not treated. When active power injection is used for POD, the area of the E-STATCOM has a full-size impact on its dynamic performance. furthermore, the standard manipulate strategy of the tool for POD available in the literature is similar to the only utilized for electricity device stabilizer (PSS) [9], wherein a chain of wash-out and lead-lag filter out hyperlinks are used to generate the manipulate enter alerts. This form of manipulate approach is powerful simplest at the working factor in which the design of the filter out hyperlinks is optimized, and its pace of reaction is confined by way of the frequency of the electromechanical oscillations. In this paper, a manage strategy for the E-STATCOM while used for POD might be investigated. Way to the selected neighborhood sign quantities measured within the system, the control approach optimizes the injection of energetic and reactive electricity to

provide uniform damping at diverse places inside the energy system. It will be proven that the applied manage algorithm is powerful in opposition to system parameter uncertainties. For this, a changed recursive least square (RLS)-based totally estimation algorithm as defined in [13], [14] may be used to extract the specified control alerts from domestically measured alerts. Subsequently, the effectiveness of the proposed control strategy can be validated through simulation and experimental verification.

## II. Static Synchronous Compensator (STATCOM):

The STATCOM is a shunt-connected VSC, showed in Figure 1. It is one of the key FACTS controllers with the ability to control the output reactive current, and hence the reactive power, independently of the AC voltage [1].

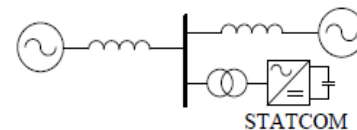


**Fig. 1 Transmission line with STATCOM**

It is mainly used for voltage control but can also be used for increasing of transmission capacity in power lines, improving the voltage/angle stability, damping of oscillations and as an active filter [6]. Furthermore, the STATCOM can be used for grid connection of renewable energy sources to fulfill the grid codes. In its basic structure, the STATCOM can only exchange reactive power with the grid, but if equipped with energy storage, the STATCOM can also exchange active power.

## III. SYSTEM MODELING FOR CONTROLLER DESIGN:

A basic power system representation in Fig. 2 is used to learn the impact of the E-STATCOM on the power system dynamics. The investigated system approximates a collective model of a two-area power system, where each area is represented by a synchronous generator.

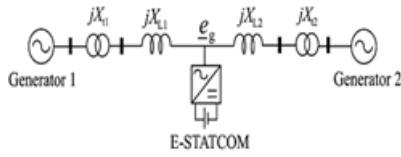


Fig.2 Simplified two-machine system with E-STATCOM.

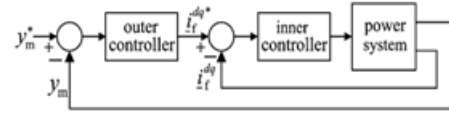


Fig. 3 Block diagram of the control of E-STATCOM

The synchronous generators are modeled as voltage sources of constant magnitude ( $V_{g1}, V_{g2}$ ) and dynamic rotor angles ( $\delta_{g1}, \delta_{g2}$ ) behind a transient reactance ( $X'_{d1}, X'_{d2}$ ). The transmission system consists of two transformers represented by their equivalent leakage reactance ( $X_{t1}, X_{t2}$ ) and a transmission line with equivalent reactance ( $X_L = X_{L1} + X_{L2}$ ). The losses in the transmission system and mechanical damping are neglected, the overall damping for the investigated system is equal to zero. Therefore, the model is appropriate to allow a conservative approach of the impact of the E-STATCOM when used for stability studies [14]. For analysis purpose, the electrical connection point of the converter along the transmission line is expressed by the parameter  $a$  as

$$a = \frac{X_1}{(X_1 + X_2)} \quad (1)$$

where

$$\begin{aligned} X_1 &= X'_{d1} + X_{t1} + X_{L1} \\ X_2 &= X'_{d2} + X_{t2} + X_{L2} \end{aligned}$$

The control of the E-STATCOM consists of an outer control loop and an inner current control loop, as shown in Fig. 3. The outer control loop, which can be an ac voltage, dc-link voltage or POD controller, sets the reference current for the inner current controller. The general measured signal  $y_m$  depends on the type of outer loop control. The control algorithm is implemented in dq-reference frame where a phase-locked loop (PLL) [15] is used to track the grid-voltage angle  $\theta_g$  from the grid-voltage vector  $e_g$ . By synchronizing the PLL with the grid-voltage vector, the d and q components of the injected current ( $i_f^d$  and  $i_f^q$ ) control the injected active and reactive power, respectively. In the notation in Fig.3, the superscript “\*” denotes the corresponding reference signals.

In this paper, the outer manipulate loop is thought to be a POD controller, and the element of the block can be described in phase III. Because of this, we assume that the injected active and reactive powers in the consistent nation are zero. Whilst designing a cascaded controller, the rate of outer control loop is generally selected to be a whole lot slower than the internal one to guarantee balance. This means that the contemporary controller can be considered infinitely rapid whilst designing the parameters of the outer controller loop. Therefore, the E-STATCOM can be modeled as a managed ideal current supply, as depicted within the equal circuit in Fig. 3, for analysis purpose.

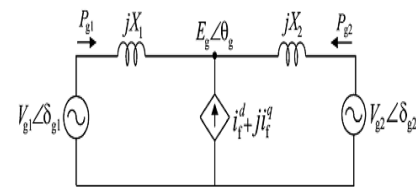


Fig. 4. Equivalent circuit for two-machine system with E-STATCOM.

The level of power oscillation damping provided by the converter depends on how much the active power output from the generators is modulated by the injected current,  $i_f$ . For the system in Fig. 4, the change in active power output from the generators due to injected active and reactive power from the E-STATCOM is calculated as in

$$\begin{aligned} \Delta P_{g1, P} &\approx -\Gamma_P P_{inj}, & \Delta P_{g2, P} &\approx -(1 - \Gamma_P) P_{inj} \\ \Delta P_{g1, Q} &\approx \left[ \frac{V_{g1} V_{g2} \sin(\delta_{g10} - \delta_{g20}) a(1-a)}{E_{g0}^2} \right] Q_{inj} \\ \Delta P_{g2, Q} &\approx - \left[ \frac{V_{g1} V_{g2} \sin(\delta_{g10} - \delta_{g20}) a(1-a)}{E_{g0}^2} \right] Q_{inj} \end{aligned} \quad (2)$$

where  $(\Delta P_{g1,P}, \Delta P_{g2,P})$  and  $(\Delta P_{g1,Q}, \Delta P_{g2,Q})$  represent the change in active power from the corresponding generators due to injected active power ( $P_{inj}$ ) and reactive power ( $Q_{inj}$ ), respectively.  $\Gamma_P$ ,  $P_{inj}$  and  $Q_{inj}$  are given by

$$\Gamma_P = \frac{((1-a)V_{g1})^2 + a(1-a)V_{g1}V_{g2} \cos(\delta_{g10} - \delta_{g20})}{E_{g0}^2}$$

$$P_{inj} \approx E_{g0}i_f^d$$

$$Q_{inj} \approx -E_{g0}i_f^d \quad (3)$$

The initial steady-state PCC voltage magnitude  $E_{g0}$  and generator rotor angles  $(\delta_{g10}, \delta_{g20})$  correspond to the operating point where the converter is in inactive mode. It can be seen from equ. (2) and (3) that the change in active power output from the generators depends on the location of the converter  $a$  as well as on the amount of injected active and reactive power. Moreover, it can be understood from equ. (2) that the effect of reactive power injection depends on the magnitude and direction of transmitted power from the generators.

#### IV. POD CONTROLLER DESIGN:

The derivative of the POD controller from locally measured signals will be made in this section.

##### A. Derivative of Control Input Signals:

Considering the simplified two-machine system in Fig. 2, the active power output from each generator should change in proportion to the change in its speed to provide damping [9]. From (2), it can be observed that the effect of the power injected by the compensator on the generator active power output highly depends on the parameter  $a$ , i.e., on the location of the E-STATCOM. Using the equivalent system in Fig. 4, a control input signal that contains information on the speed variation of the generators can be derived. When the E-STATCOM is not injecting any current, the variation of the locally measured signals,  $\theta_g$  and  $P_{tran}$  at different E-STATCOM connection points using the dynamic generator rotor angles  $\delta_{g1}$  and  $\delta_{g2}$  is given by

$$\theta_g = \delta_{g2} + \tan^{-1} \left[ \frac{(1-a)V_{g1} \sin(\delta_{g1} - \delta_{g2})}{(1-a)V_{g1} \cos(\delta_{g1} - \delta_{g2}) + aV_{g2}} \right] \quad (4)$$

$$P_{tran} = \frac{V_{g1}V_{g2} \sin(\delta_{g1} - \delta_{g2})}{X_1 + X_2} \quad (5)$$

From a small-signal point of view and under the statement that the PCC-voltage magnitude along the line  $E_g$  does not change considerably, the required control input signals can be derived from the PCC-voltage phase and transmitted active power as [14]

$$\frac{d\theta_g}{dt} \approx \Gamma_P \omega_{g0} \Delta\omega_{g1} + (1 - \Gamma_P) \omega_{g0} \Delta\omega_{g2} \quad (6)$$

$$\frac{dP_{tran}}{dt} \approx \left\{ \frac{V_{g1}V_{g2} \cos(\delta_{g10} - \delta_{g20})}{X_1 + X_2} \right\} \omega_{g0} [\Delta\omega_{g1} - \Delta\omega_{g2}] \quad (7)$$

where the constant  $\Gamma_P$  has been defined in the previous section. The nominal system frequency is represented by  $\omega_{g0}$  whereas  $\Delta\omega_{g1}$  and  $\Delta\omega_{g2}$  represent the speed variation of the generators in p.u. The electromechanical dynamics for each generator [ $i = 1, 2$ ] is given by [9]

$$2H_{gi} \frac{d\Delta\omega_{gi}}{dt} = \Delta T_{mi} - \Delta T_{gi} - K_{Dmi} \Delta\omega_{gi} \quad (8)$$

where  $H_{gi}$ ,  $\Delta\omega_{gi}$ ,  $\Delta T_{mi}$ ,  $\Delta T_{gi}$ , and  $K_{Dmi}$  represent inertia constant, speed variation, change in input torque, change in torque and mechanical damping constant for the  $i$ th generator respectively. The derivative of the PCC-voltage section and transmitted active power are each depending on the speed variation of the generators. Moreover, the spinoff of the PCC-voltage phase relies upon on the place of E-STATCOM, thru the parameter  $\Gamma_P$ , as well as the mechanical dynamics of the generators as proven in (8). This information can be exploited in the POD controller design. For the two machine system in Fig. 3, damping is related to the variation of the speed difference between the two generators,  $\Delta\omega_{g12} = \Delta\omega_{g1} - \Delta\omega_{g2}$ . From (2) and (3), it can be understood that the change in the output power from the generators due to injected active power is maximum when the compensator is installed at the

generator terminals (i.e.  $a = 0$  and  $a = 1$ ). Assuming equal inertia constant for the two generators, no damping is provided by injection of active power at the electrical midpoint of the line (i.e.,  $a = 0.5$  for  $H_{g1} = H_{g2}$ ) as the power output of the two generators is the same and the net impact is zero. At this location, the derivative of PCC-voltage phase is zero [see (6)]. This means that  $d\theta_g/dt$  scales the speed variation of the two generators depending on the location of E-STATCOM and its magnitude changes in proportion to the level of damping by active power injection. Therefore  $d\theta_g/dt$  is an appropriate input signal for controlling the active power injection. On the other hand, it can be understood from (2) that the change in the output power from the generators due to injected reactive power is maximum at the electrical midpoint of the line (i.e.,  $a = 0.5$ ) and minimum at the generator terminals (i.e.,  $a = 0$  and  $a = 1$ ). As the changes in the power output of the two generators are the same in magnitude and opposite in sign, a signal that varies linearly with the speed variation between the two generators,  $\Delta\omega_{g12}$  is a suitable signal to control reactive power injection. This information can be obtained from the derivative of the transmitted active power  $dP_{tran}/dt$ .

**B. Estimation of Control Input Signals:**

As described in the Introduction, effective power oscillation damping for various power system operating points and E-STATCOM locations require fast, accurate, and adaptive estimation of the critical power oscillation frequency component. This is achieved by the use of an estimation method used on a modified RLS algorithm. For reasons described in the previous subsection, the derivative of the PCC-voltage phase and the transmitted power should be estimated for controlling the active and reactive power injection, correspondingly. The aim of the algorithm is therefore to estimate the signal components that consist of only the low-frequency electromechanical oscillation in the measured signals  $\theta_g$  and  $P_{tran}$ . By using a PLL with bandwidth much higher than the frequency of electromechanical oscillations, the derivative of the PCC-voltage phase can be obtained from the change in

frequency estimate of the PLL ( $\Delta\tilde{\omega}_g = d\theta_g/dt$ ). Therefore, the low-frequency electromechanical oscillation component can be extracted directly from the frequency estimate of the PLL. On the other hand, the derivative of transmitted power is estimated by extracting the low-frequency electromechanical oscillation component from the measured signal,  $P_{tran}$  and then applying a phase shift of  $\pi/2$  to the estimated oscillation frequency component. From the estimated control input signals  $\tilde{\omega}_{g,osc} = d\tilde{\omega}_{g,osc}/dt$  and  $d\tilde{P}_{tran,osc}/dt$ , which hold only a particular oscillation frequency component, the reference injected active and reactive current components ( $i_f^{d*}, i_f^{q*}$ ) from the E-STATCOM can be calculated to group the POD controller as shown in Fig.5. The terms  $K_P$  and  $K_Q$  represent proportional controller gains for the active and reactive current components, respectively. To describe the estimation algorithm, an input signal  $y$  which could be either  $\tilde{\omega}_g$  or  $P_{tran}$ , as shown in Fig.5, is considered. Following a power system disturbance,  $y$  will consist of an average value that varies slowly and a number of low-frequency oscillatory components, depending on the number of modes that are excited by the disturbance. For simplicity, let us assume that there exist single oscillatory components in the input signal. Therefore, the input signal consists of an average component  $Y_{avg}$  and an oscillatory component  $Y_{osc}$  which can be modeled as

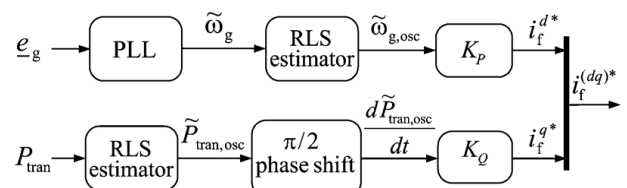


**Fig. 5 Block diagram of the POD controller.**

$$y(t) = Y_{avg}(t) + Y_{ph}(t)\cos[\omega_{osc}t + \varphi(t)] \tag{9}$$

where  $Y_{osc}$  is expressed in terms of its magnitude ( $Y_{ph}$ ), frequency ( $\omega_{osc}$ ) and phase( $\varphi$ ). The model in (9) is rewritten using the oscillation angle  $\theta_{osc}(t) = \omega_{osc}t$  as  $y(t) = Y_{avg}(t) + Y_{ph,d}(t)\cos(\theta_{osc}(t)) - Y_{ph,q}(t)\sin(\theta_{osc}(t))$  where the terms  $P_{ph,d}$  and  $P_{ph,q}$  are given by  $Y_{ph,d}(t) = Y_{ph}(t)\cos(\varphi(t))$   $Y_{ph,q}(t) = Y_{ph}(t)\sin(\varphi(t))$ .

From an observation matrix  $\Phi$  and measured input signal  $y(t)$ , the estimated state vector  $\tilde{h}$  is derived using the RLS algorithm in discrete time as [13],[14]

$$\tilde{h}(k) = \tilde{h}(k-1) + G(k)[y(k) - \Phi(k)\tilde{h}(k-1)] \quad (10)$$

with

$$\begin{aligned} \tilde{h}(k) &= [\tilde{Y}_{avg}(k) \quad \tilde{Y}_{ph,d}(k) \quad \tilde{Y}_{ph,q}(k)]^T \\ \Phi(k) &= [1 \quad \cos(\theta_{osc}(t)) \quad -\sin(\theta_{osc}(t))]. \end{aligned}$$

Calling  $I$  the identity matrix, the gain matrix  $G$  and covariance matrix  $R$  are calculated recursively starting with an initial invertible matrix  $R(0)$  as

$$G(k) = R(k-1)\Phi^T(k)[\lambda + \Phi(k)R(k-1)\Phi^T(k)]^{-1} \quad (11)$$

$$R(k) = \frac{[I - G(k)\Phi(k)]R(k-1)}{\lambda} \quad (12)$$

where  $\lambda$  represents the forgetting factor for the RLS algorithm such that  $0 < \lambda \leq 1$ . With  $T_s$  representing the sampling time, the steady-state bandwidth of the RLS  $\alpha_{RLS}$  and the estimation error  $\epsilon(k)$  are given by [14]

$$\alpha_{RLS} = \frac{(1-\lambda)}{T_s}, \quad \epsilon(k) = y(k) - \Phi(k)\tilde{h}(k-1)$$

**Modification in the Conventional RLS Algorithm:**

The selection of  $\alpha_{RLS}$  is an exchange among a terrific selectivity for the estimator and its speed of response [13], [14]. A high forgetting factor effects in low estimation velocity with properly frequency selectivity. With increasing estimation pace (reducing  $\lambda$ ), the frequency selectivity of the set of rules reduces. Because of this, the conventional RLS set of rules ought to be modified which will acquire rapid temporary estimation without compromising its consistent-state selectivity.

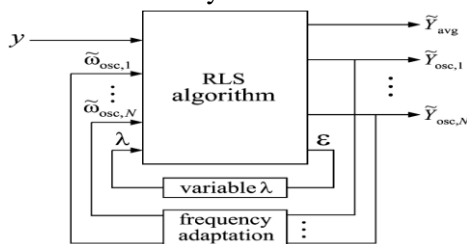


**Fig. 6. Block diagram of the modified RLS estimator for multiple oscillation modes**

In this paper, this is achieved with the use of variable forgetting factor as described in [13]. When the RLS algorithm is in steady-state, its bandwidth is determined by the steady-state forgetting factor ( $\lambda_{ss}$ ). If a rapid change is detected in the input (i.e., if the estimation error magnitude,  $|\epsilon(k)|$  exceeds a predefined threshold),  $\lambda$  will be modified to a smaller transient forgetting factor ( $\lambda_{tr}$ ). Thus, by using a high-pass filter with time constant  $\tau_{hp}$ ,  $\lambda$  will be slowly increased back to its steady-state value  $\lambda_{ss}$ . Besides  $\lambda$ , the performance of the estimation method depends on accurate knowledge of the oscillating frequency,  $\omega_{osc}$ . This frequency is dependent on the system parameters and its operating conditions. If the frequency content of the input changes, the estimator will give rise to a phase and amplitude error in the estimated quantities. Therefore, a frequency adaptation mechanism as described in [14] is implemented to track the true oscillation frequency of the input from the estimate of the oscillatory component,  $\tilde{Y}_{osc}$ .

**Modification for Multiple Oscillation Modes:**

The investigated manipulate technique has been derived beneath the assumption of an unmarried oscillatory frequency factor in the enter sign. A quick description of how the proposed set of rules may be extended for multi-location machine with multiple oscillation modes could be in short presented right here for destiny reference. Assuming that the input signal  $y$  contains  $N$  oscillatory additives, (9) ought to be modified as

$$\begin{aligned} y(t) &= Y_{avg}(t) + \sum_{i=1}^N Y_{osc} \\ &= Y_{avg}(t) + \sum_{i=1}^N Y_{ph,i}(t)\cos[\omega_{osc,i}t + \phi_i(t)] \end{aligned} \quad (13)$$

where the  $i_{th}$  oscillation mode  $Y_{osc,i}$  (with  $i=1, \dots, N$ ) is expressed in terms of its amplitude ( $Y_{ph,i}$ ), frequency ( $\omega_{osc,i}$ ), and phase ( $\phi_i$ ). Using the model in (13), the RLS described in the previous section (including variable forgetting factor and frequency adaptation for each considered oscillation mode) can be modified as described in Fig.5.

Thus, the POD controller in Fig.4 can be modified so to control each mode independently. Observe that the phase-shift applied for calculation of the reference currents depends on the investigated system and needs to be calculated for each oscillatory mode [9].

## V. STABILITY ANALYSIS OF SYSTEM MODEL:

The mathematical model of the system in Fig.4 is developed in this section to examine the performance of the POD controller using active and reactive power injection. Using the expressions in (6)-(7) for  $d\theta_g/dt$  and  $dP_{tran}/dt$ , the injected currents are controlled as

$$i_f^d \approx K_P \omega_{g0} [\Gamma_P \Delta \omega_{g1} + (1 - \Gamma_P) \Delta \omega_{g2}] \quad (14)$$

$$i_f^q \approx K_Q \omega_{g0} \left\{ \frac{V_{g1} V_{g2} \cos(\delta_{g10} - \delta_{g20})}{X_1 + X_2} \right\} [\Delta \omega_{g1} - \Delta \omega_{g2}] \quad (15)$$

Where the constant  $\Gamma_P$  is as defined in (3). Linearizing around an initial steady-state operating point, the small-signal dynamic model of the two-machine system with the E-STATCOM in per unit is developed as in

$$\frac{d}{dt} \begin{bmatrix} \Delta \omega_{g1} \\ \Delta \delta_{g12} \\ \Delta \omega_{g2} \end{bmatrix} = \begin{bmatrix} \beta_{11} & \beta_{12} & \beta_{13} \\ \omega_{g0} & 0 & -\omega_{g0} \\ \beta_{31} & \beta_{32} & \beta_{33} \end{bmatrix} \begin{bmatrix} \Delta \omega_{g1} \\ \Delta \delta_{g12} \\ \Delta \omega_{g2} \end{bmatrix} + \begin{bmatrix} 1 \\ 2H_{g1} \\ 0 \\ 0 \\ 1 \\ 2H_{g2} \end{bmatrix} \begin{bmatrix} \Delta T_{m1} \\ \Delta T_{m2} \end{bmatrix} \quad (16)$$

where  $\Delta \delta_{g12} = \Delta \delta_{g1} - \Delta \delta_{g2}$  represents the rotor angle difference between the two generators and other signals as defined previously. Assuming no mechanical damping and the initial steady-state speed of the generators set to  $\omega_{g0}$ , the constants are derived as in

$$\begin{bmatrix} \beta_{11} \\ \beta_{12} \\ \beta_{13} \\ \beta_{31} \\ \beta_{32} \\ \beta_{33} \end{bmatrix} = \begin{bmatrix} \frac{\omega_{g0}(K_P E_{g0} \Gamma_P^2 + K_Q \Gamma_Q)}{2H_{g1}} \\ -\frac{V_{g1} V_{g2} \cos(\delta_{g10} - \delta_{g20})}{2H_{g1}(X_1 + X_2)} \\ \frac{\omega_{g0}(K_P E_{g0} \Gamma_P (1 - \Gamma_P) - K_Q \Gamma_Q)}{2H_{g1}} \\ \frac{\omega_{g0}(K_P E_{g0} \Gamma_P (1 - \Gamma_P) - K_Q \Gamma_Q)}{2H_{g2}} \\ \frac{V_{g1} V_{g2} \cos(\delta_{g10} - \delta_{g20})}{2H_{g2}(X_1 + X_2)} \\ \frac{\omega_{g0}(K_P E_{g0} (1 - \Gamma_P)^2 - K_Q \Gamma_Q)}{2H_{g2}} \end{bmatrix}$$

(17)

Where  $\Gamma_Q$  is given by

$$\Gamma_Q = \frac{[V_{g1} V_{g2}]^2 \sin(2(\delta_{g10} - \delta_{g20})) a(1-a)}{2E_{g0}(X_1 + X_2)} \quad (18)$$

The terms  $\beta_{12}$  and  $\beta_{32}$  represent the synchronizing torque coefficients resulting from the selected operating point and the contribution of the E-STATCOM is zero. The terms  $\beta_{11}$  and  $\beta_{33}$  determine the damping torque coefficient provided by the E-STATCOM with respect to the change in speed of the respective generator. To provide positive damping,  $\beta_{11}$  and  $\beta_{33}$  should be negative. For this, the sign of  $K_P$  should be negative and the sign of  $K_Q$  should be chosen based on the sign of  $\Gamma_Q$ . For a transmitted power from Generator 1 to Generator 2,  $\Gamma_Q$  will be positive and the sign of  $K_Q$  should be negative. For a transmitted power in the other direction, the sign of  $K_Q$  should be opposite. The terms  $\beta_{13}$  and  $\beta_{31}$  are the cross coupling terms between the two generator speed variations. With active power injection only ( $K_Q = 0$ ), the cross coupling terms reduce the damping as the speed variation of the generators will be opposite at the oscillatory frequency. At the mass-scaled electrical midpoint of the line where  $d\theta_g/dt = 0$ , the damping that can be provided by  $P_{inj}$  is zero. Therefore, the active power injected by the E-STATCOM at this location is set to zero by the control algorithm. When moving away from this point towards the generator terminals,  $\Gamma_P$  increases and at the same time the cross coupling terms decrease.

This enhances the damping that can be provided by active power injection and therefore the amount of injected active power is increased. In the case of reactive power injection only ( $K_p = 0$ ), positive damping is provided by the cross coupling terms and maximum damping is provided at the electrical midpoint of the line (i.e.,  $a = 0.5$  for a symmetrical system) where  $\Gamma_Q$  magnitude is maximum.

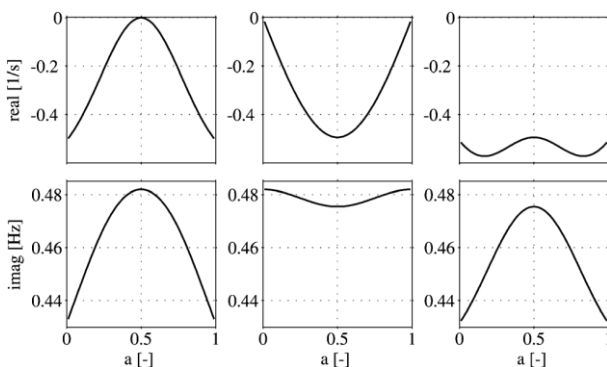


**Fig. 7. Real and imaginary part of the complex conjugate poles versus position. (a) Active power injection. (b) Reactive power injection. (c) Active and reactive power injection. [ $K_p = -0.08$ ,  $K_Q = -0.34$ ,  $P_{tran} = 0.4444$  p.u.].**

As an example for the analysis in this section, a hypothetical 20/230 KV, 900 MVA transmission system similar to the one in Fig. 2 with a total series reactance of 1.665 p.u. and inertia constant of the generators  $H_{g1} = H_{g2} = 6.5s$  is considered. The leakage reactance of the transformers and transient impedance of the generators are 0.15 p.u. and 0.3 p.u., respectively. The movement of the poles for the system as a function of the E-STATCOM location is shown in Fig. 7. With the described control strategy, injected active power is zero at the point where the effect of active power injecting on damping is zero. This is at the electrical midpoint of the line. On the other hand, at the same location damping by the reactive power injection is maximum. The reverse happens at either end of the generators. Thanks to a good control of  $P_{inj}$  and  $Q_{inj}$ , it is also possible to see from Fig. 7 that a more uniform damping along the line is obtained by using injection of both active and reactive power.

## VI FUZZY LOGIC CONTROLLER:

In FLC, simple control motion is determined by a fixed of linguistic policies. These policies are determined by the gadget. Because the numerical variables are transformed into linguistic variables, mathematical modeling of the machine isn't always required in FC. The FLC contains of 3 parts: fuzzification, inference engine and defuzzification. The FC is characterised as

- i. Seven fuzzy units for every enter and output.
- ii. Triangular membership functions for simplicity.
- iii. Fuzzification the usage of continuous universe of discourse.
- iv. Implication the use of Mamdani's, 'min' operator.
- v. Defuzzification the usage of the height approach.

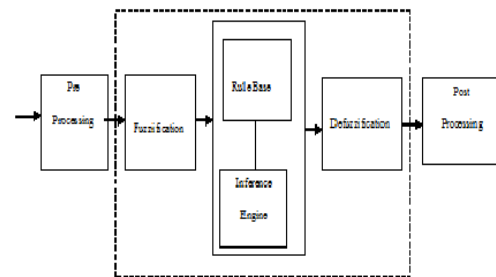


**Fig.8 Fuzzy logic controller**

### Fuzzification:

Membership function values are assigned to the linguistic variables, using seven fuzzy subsets: NB (Negative Big), NM (Negative Medium), NS (Negative Small), ZE (Zero), PS (Positive Small), PM (Positive Medium), and PB (Positive Big). The partition of fuzzy subsets and the shape of membership CE(k) E(k) function adapt the shape up to appropriate system. The value of input error and change in error are normalized by an input scaling factor In this system the input scaling factor has been designed such that input values are between -1 and +1. The triangular shape of the membership function of this arrangement presumes that for any particular E(k) input there is only one dominant fuzzy subset. The input error for the FLC is given as

$$E(k) = \frac{P_{ph}(k) - P_{ph}(k-1)}{V_{ph}(k) - V_{ph}(k-1)} \quad (14)$$

$$CE(k) = E(k) - E(k-1) \tag{15}$$

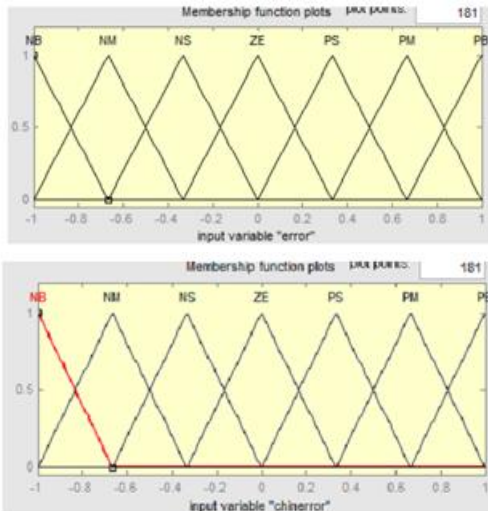


**Fig.9 Membership functions**

Change In Error	Error						
	NB	NM	NS	Z	PS	PM	PB
NB	PB	PB	PB	PM	PM	PS	Z
NM	PB	PB	PM	PM	PS	Z	Z
NS	PB	PM	PS	PS	Z	NM	NB
Z	PB	PM	PS	Z	NS	NM	NB
PS	PM	PS	Z	NS	NM	NB	NB
PM	PS	Z	NS	NM	NM	NB	NB
PB	Z	NS	NM	NB	NB	NB	NB

Table1. Fuzzy Rules

**Inference Method:**

Several composition methods such as Max–Min and Max–Dot have been proposed in the literature. In this paper Min method is used. The output membership function of each rule is given by the minimum operator and maximum operator. Table 1 shows rule base of the FLC.

**Defuzzification:**

As a plant commonly requires a non-fuzzy value of manipulate, a defuzzification stage is needed. To compute the output of the FLC, height approach is used and the FLC output modifies the manipulate output. Similarly, the output of FLC controls the switch inside the inverter. In UPQC, the active power, reactive power, terminal voltage of the line and capacitor voltage are required to be maintained. So that it will control these parameters, they are sensed and as

compared with the reference values. To reap this, the membership functions of FC are: mistakes, exchange in error and output.

The set of FC rules are derived from  $u = -[\alpha E + (1-\alpha)*C]$

Where  $\alpha$  is self-adjustable factor which can regulate the whole operation. E is the error of the system, C is the change in error and u is the control variable. A large value of error E indicates that given system is not in the balanced state. If the system is unbalanced, the controller should enlarge its control variables to balance the system as early as possible. set of FC rules is made using Fig.(b) is given in Table 1.

**THE MEMBERSHIP FUNCTION EDITOR:**

The membership feature Editor shares a few features with the FIS Editor. In truth, all of the 5 simple GUI gear have comparable menu alternatives, fame lines, and help and near buttons. The membership feature Editor is the tool that helps you to display and edits all of the club features related to all of the input and output variables for the complete fuzzy inference gadget. Fig. 9 suggests the club characteristic Editor. You could first use the mouse to pick a specific membership characteristic related to a given variable excellent, (including poor, for the variable, provider), and then drag the club characteristic to and fro. This could affect the mathematical description of the high-quality associated with that club function for a given variable. the chosen membership characteristic can also be tagged for dilation or contraction via clicking at the small square drag points at the club function, and then dragging the characteristic with the mouse towards the out of doors, for dilation, or toward the interior, for contraction. This will alternate the parameters related to that club feature.

1. Curve to rancid. To alter the shape of the club function, either uses the mouse, as defined above or kind in a desired parameter change, and then click on the club function. The default parameter listing for this curve is [0 0 1 3].

2. Name the curve with the rightmost trapezoid, delicious, and reset the related parameters if preferred.

**VII. SIMULATION RESULTS:**

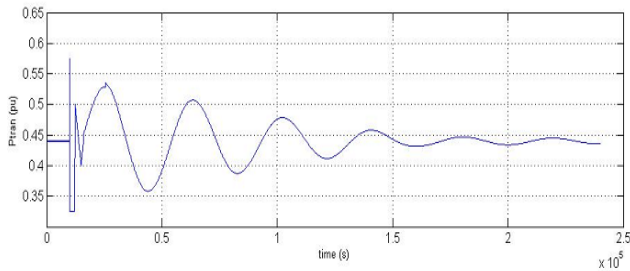


**Fig.1 (a) Calculated transmitted active power output following a three-section fault with E-STATCOM linked at bus 7 POD by  $P_{inj}$ .**

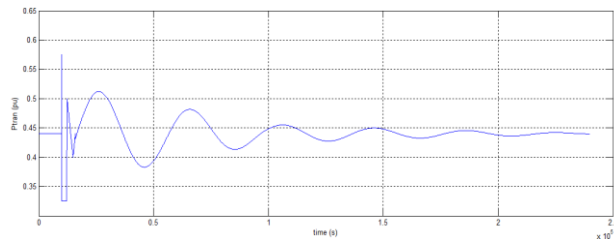


**Fig.1 (b) Calculated transmitted active power output following a three-section fault with E-STATCOM linked at bus 7 POD by  $P_{inj}$  and  $Q_{inj}$**

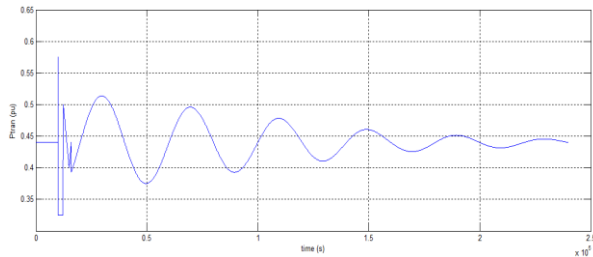


**Fig.1(c) Calculated transmitted active power output following a three-section fault with E-STATCOM linked at bus 7 POD by  $Q_{inj}$**

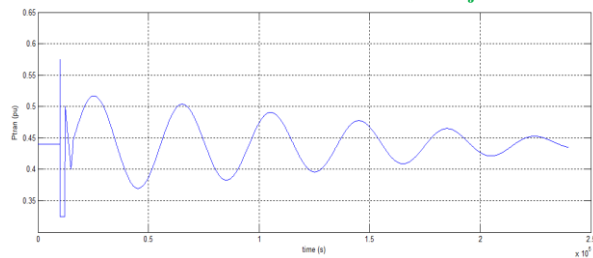


**Fig. 1(d) Calculated transmitted active power output following a three-section fault with E-STATCOM linked at bus 7 without POD**

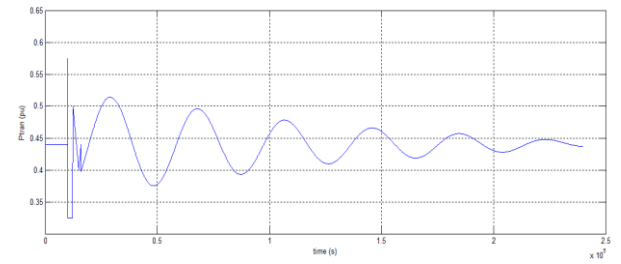


**Fig.2 (a) Calculated transmitted active power output following a three-section fault with E-STATCOM linked at bus 8 POD by  $P_{inj}$**

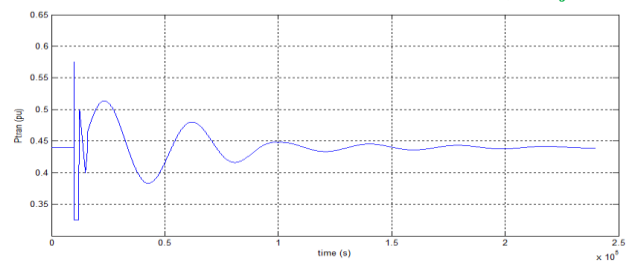


**Fig. 2 (b) Calculated transmitted active power output following a three-section fault with E-STATCOM linked at bus 8 POD by  $P_{inj}$  and  $Q_{inj}$**

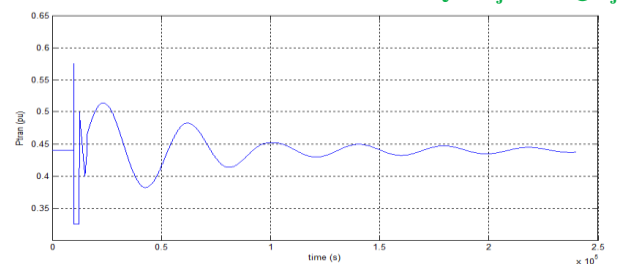


**Fig. 2 (c) Calculated transmitted active power output following a three-section fault with E-STATCOM linked at bus 8 POD by  $Q_{inj}$ .**

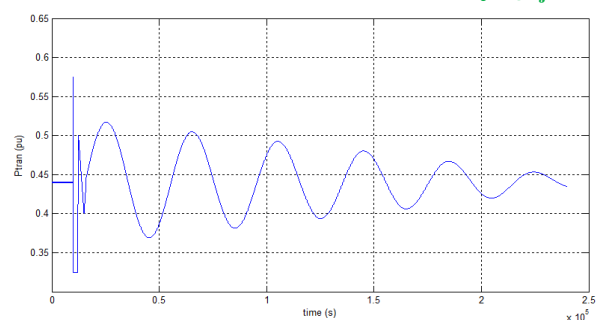


**Fig. 2 (d) Calculated transmitted active power output following a three-section fault with E-STATCOM linked at bus 8 without POD.**

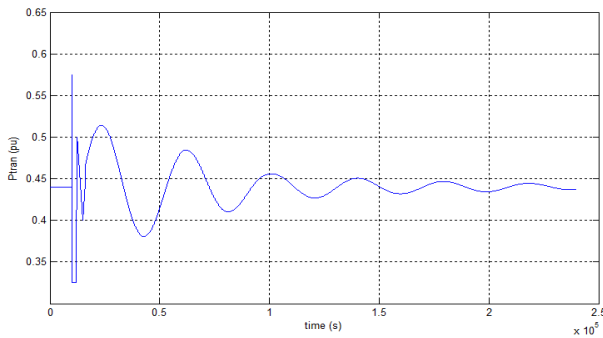


**Fig. 3 (a)** Calculated transmitted active power output following a three-section fault with E-STATCOM linked at bus 9 POD by  $P_{inj}$ .

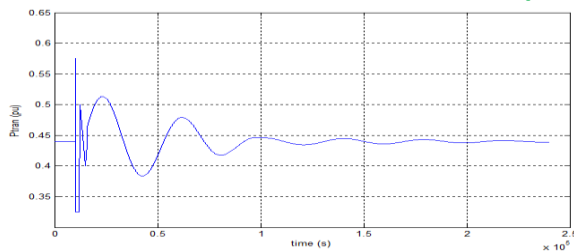


**Fig. 3 (b)** Calculated transmitted active power output following a three-section fault with E-STATCOM linked at bus 9 POD by  $P_{inj}$  and  $Q_{inj}$

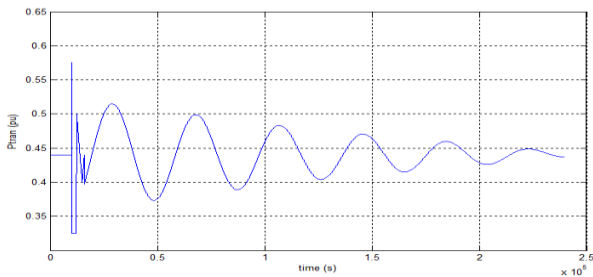


**Fig. 3 (c)** Calculated transmitted active power output following a three-section fault with E-STATCOM linked at bus 9 POD by  $Q_{inj}$

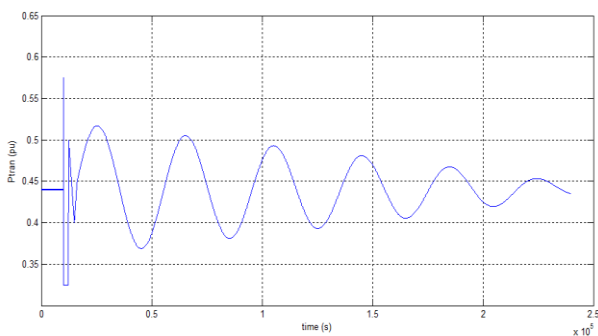


**Fig. 3 (d)** Calculated transmitted active power output following a three-section fault with E-STATCOM linked at bus 9 without POD.

The POD controller described in Section IV is here verified simulation using the well known two-area four-machine system in Fig. 11.

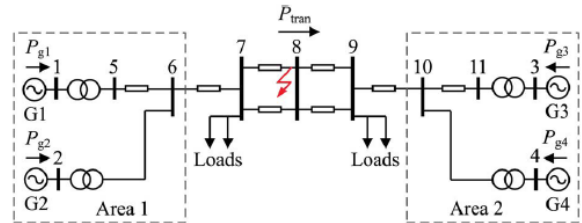


**Fig. 11.** Simplified two-area four machine power system

The applied device is rated 20/230 KV, 900 MVA and the parameters for the mills and transmission gadget collectively with the loading of the device are given in element in [9]. The machine is initially working in constant-country with a transmitted active power,  $P_{tran} = 400\text{MW}$  from area 1 to location 2. A 3-section fault is implemented to the system on one of the transmission traces among bus 7 and bus 8. The fault is cleared after 120ms with the aid of disconnecting the faulted line. Because of the carried out disturbance, a poorly damped oscillation is obtained after the fault clearing. With the POD controller shape defined in Fig. 5, the overall performance of the E-STATCOM following the fault at 3 unique locations is proven in Fig. 10.

As described inside the small-signal analysis for two-machine system device in section-V, whilst moving toward the generator devices, a better damping is finished by way of active power injection. With admire to reactive power injection, maximum damping action is supplied while the E-STATCOM is attached near the electrical midpoint of the line and the level of damping decreases when moving far away from it. Due to an amazing alternative of alerts for controlling both active and reactive power injection, powerful power oscillation damping is furnished via the E-STATCOM no matter its region inside the line.

## VIII. CONCLUSION:

An adaptive POD controller with the aid of E-STATCOM has been advanced on this paper. For this, a modified RLS set of rules has been used for estimation of the low-frequency electromechanical oscillation additives from locally measured indicators all through energy machine disturbances. The estimator enables a fast, selective and adaptive estimation of signal additives at the power oscillation frequency. The dynamic performance of the POD controller to provide powerful damping at numerous connection points of the E-STATCOM has been demonstrated through simulation. The robustness of the manipulate algorithm in opposition to machine parameter changes has also been verified through experimental exams. Furthermore, the usage of the frequency version at the E-STATCOM connection factor because the enter sign for the active power modulation, it has been shown that active power injection is minimized at factors in the strength device in which its impact on POD is negligible. These consequences in a most effective use of the available strength supply.

## REFERENCES:

- [1] N. G. Hingorani and L. Gyugyi, Understanding FACTS. Concepts and Technology of Flexible AC Transmission Systems. New York, NY, USA: IEEE, 2000.
- [2] G. Cao, Z. Y. Dong, Y. Wang, P. Zhang, and Y. T. Oh, "V SC based STATCOM controller for damping multi-mode oscillations," in Proc. IEEE Power and Energy Soc. General Meeting—Conversion and Delivery of Electrical Energy in the 21st Century, Jul. 2008, pp. 1–8.
- [3] M. Zarghami and M. L. Crow, "Damping inter-area oscillations in power systems by STATCOMs," in Proc. 40th North Amer. Power Symp., Sep. 2008, pp. 1–6.
- [4] Z. Yang, C. Shen, L. Zhang, M. L. Crow, and S. Atcitty, "Integration of a statcom and battery energy storage," IEEE Trans. Power Syst., vol. 16, no. 2, pp. 254–260, May 2001.
- [5] A. Arulampalam, J. B. Ekanayake, and N. Jenkins, "Application study of a STATCOM with energy storage," Proc. Inst. Electr. Eng.—Gener., Transm. and Distrib., vol. 150, pp. 373–384, July 2003.
- [6] N. Wade, P. Taylor, P. Lang, and J. Svensson, "Energy storage for powerflow management and voltage control on an 11 kV UK distribution network," Prague, Czech Republic, CIRED paper 0824, Jun. 2009.
- [7] [7] A. Adamczyk, R. Teodorescu, and P. Rodriguez, "Control of full-scale converter based wind power plants for damping of low frequency system oscillations," in Proc. IEEE PowerTech, Trondheim, Norway, Jun. 2011, pp. 1–7.
- [8] H. Xie, "Onpower-system benefits, main-circuit design, control of Statcoms with energy storage," Ph.D. dissertation, Dept. Electr. Energy Conversion, Royal Inst. Technol., Stockholm, Sweden, 2009.
- [9] P. Kundur, Power System Stability and Control. New York, NY, USA: McGraw-Hill, 1994.
- [10] K. Kobayashi, M. Goto, K. Wu, Y. Yokomizu, and T. Matsumura, "Power system stability improvement by energy storage type STATCOM," in Proc. IEEE Power Tech Conf., Bologna, Italy, Jun. 2003, vol. 2, DOI 10.1109/PTC.2003.1304302.
- [11] L. Zhang and Y. Liu, "Bulk power system low frequency oscillation suppression by FACTS/ESS," in Proc. IEEE PES Power Syst. Conf. Exp., Oct. 2004, pp. 219–226.
- [12] A. Arsoy, L. Yilu, P. F. Ribeiro, and F. Wang, "Power converter and SMES in controlling power system dynamics," in Proc. Ind. Appl. Conf., Oct. 2000, vol. 4, pp. 2051–2057.
- [13] M. Beza and M. Bongiorno, "A fast estimation algorithm for low-frequency oscillations in power systems," in Proc. 14th Eur. Conf. Power Electron. Appl., Sep. 2011, pp. 1–10.
- [14] M. Beza, "Control of energy storage equipped shunt-connected converter for electric power system stability enhancement," Licentiate Thesis, Dept. Energy and Environment, Chalmers Univ. of Technol., Gothenburg, Sweden, 2012.

**Author's Profile:**

**Y.Sai Krishna** had received Bachelor's degree in Electrical & Electronics Engineering from AVS College of Engineering & Technology in 2011 and he is pursuing Master's degree in Electrical Power Systems in Audisankara College of Engineering & Technology (Autonomous) Gudur, SPSR Nellore (DT), and Andhra Pradesh, India. His area of interest in Electrical Machines, Non-conventional energy sources in power systems.

**Boothapati Anil Kumar**, received B.Tech in Electrical & Electronics Engineering from Jawaharlal Nehru Technological University, Hyderabad in 2007 and M.Tech in Electrical Power Systems from Jawaharlal Nehru Technological University, Ananthapuramu in 2013. He is working as Assistant Professor in Audisankara College of Engineering & Technology since 2007. His research interest includes Power System Stability, FACTS, HVDC system and Electrical Machines.